



Original article

Comparison of Adsorption Isotherm Models for Methane and Carbon Dioxide Adsorption onto Activated Carbon

Lütfi Erden ^{a,*} & Hanife Erden ^b

^a Department of Electricity and Energy, Çan Vocational School, Çanakkale Onsekiz Mart University, Çan, Çanakkale, Türkiye

^b Department of Chemical Engineering, Faculty of Engineering, Çanakkale Onsekiz Mart University, Çanakkale, Türkiye

Abstract

Modeling and simulation of an adsorption-based gas separation process require accurately measured gas adsorption isotherms and isotherm model fittings. In this study, adsorption equilibria data of pure Methane (CH₄) and Carbon Dioxide (CO₂) onto activated carbon adsorbent (Calgon Co.) were extracted from the literature. Each experimental isotherm was correlated by the Simple Langmuir (SL), Dual Process Langmuir (DPL), Three Process Langmuir (TPL), Toth, and the Unilan models and the deviations were evaluated. Other than SL, all four models showed very good agreement with the experimental data. The fitting parameters for all models presented in this article can be used for any type of adsorption-based separation modeling which includes the BPL-activated carbon and analyzed gases.

Keywords: Adsorption Isotherm Models, CH₄ adsorption, CO₂ adsorption, Activated Carbon.

Received: 25 January 2023 * **Accepted:** 08 February 2023 * **DOI:** <https://doi.org/10.29329/ijiasr.2023.524.3>

* Corresponding author:

Erden Lütfi is an assistant professor in Çan Vocational School, Department of Electricity and Energy, Çanakkale Onsekiz Mart University, Çan, Çanakkale, Turkey. His research interests include the gas separation, gas adsorption, adsorption-based separation process design, CO₂ capture, CH₄ enrichment, Landfill gas. He currently lives and works in Çanakkale, Türkiye.
Email: lutfi.erden@comu.edu.tr

INTRODUCTION

Adsorption-based gas separation and purification have been widely used in industry for air separation, CO₂ sequestration, Argon recovery, and hydrogen or methane purification. Pressure Swing Adsorption (PSA) is one of the most attractive options in those technologies because of its low energy requirements and low capital investment costs. Adsorbent selection plays a key role in the PSA process. (Chouikhi et al., 2020; Dolan & Michael J. Mitariten, 2003; Fouladi et al., 2020; Park et al., 2020; Reynolds et al., 2006; Ribeiro et al., 2008; Ruthven et al., 1994; Santos et al., 2007; Yang, 1997)

The adsorption-based gas separation and purification techniques employ a variety of adsorbents. Among the other adsorbents used in industry, activated carbon has a very complex structure but its high surface area and micropore volume provide it with outstanding adsorbent characteristics. (Do, 1998). Activated carbon is widely used in adsorption separation processes as a result of its attractive adsorption properties (Dantas et al., 2011; Sircar et al., 1996; Sircar & Golden, 2000; Tagliabue et al., 2009).

Before performing adsorption simulations, precise data on adsorption isotherms should be acquired. Isotherm data can be measured by gravimetric, volumetric, and chromatographic techniques. In the case of high-pressure isotherm measurements, the gravimetric technique is more reliable due to the direct measurements of adsorbed mass (Belmabkhout et al., 2004).

The simulation studies prior to pilot scale or industrial scale processes can save time and money. It is very crucial to have accurate information before starting a simulation. The adsorption isotherm data then must be modeled using some empirical equations in order to use them in computer simulations. There are many adsorption isotherm models developed and used in literature in this regard. Langmuir and more sophisticated versions of Langmuir are by far the most famous adsorption isotherm models used in the literature. The Langmuir isotherm assumes monolayer coverage of adsorbate with the surface of the adsorbent having homogeneous sites with constant adsorption energy over all these sites. The DPL and TPL models are more sophisticated versions of the Simple Langmuir model with the presumption that the free energy of the adsorbate-adsorbent on each site is constant. It depicts the adsorption of a gas on a heterogeneous adsorbent made up of two and three energetically distinct but homogeneous sites. On the other hand, the Toth models were created in order to broaden the use of the Langmuir model in heterogeneous systems (Toth, 1971). It is assumed that the adsorption energies of the majority of adsorption sites are less than the mean energy (Ho et al., 2002). The parameter t deviation further away from unity indicates that the adsorption system is more heterogeneous (Do, 1998). It converges to the Simple Langmuir model when t equals one, which emphasizes the system is homogeneous.

Unilan equations are empirical equations that describe adsorption on heterogeneous surfaces by assuming a heterogeneous surface and a site yield energy distribution that is nearly continuous. The greater the value of parameter s , the more heterogeneous the system (Do, 1998).

In this study, the extracted experimental data were fitted with the Simple Langmuir (SL), Dual Process Langmuir (DPL), Three Process Langmuir (TPL), Toth, and Unilan models. Fitting performance and corresponding fitting parameters were investigated for all models. The coefficients of determination (R^2) values were also evaluated at each temperature. These findings can help with the design of various adsorption systems that use BPL-activated carbon and CH_4 or CO_2 gases. The findings of this study can also be applied to the assessment of the adsorption potential of newly developed adsorbents.

METHODS

Experimental

Experimental data from other works of the authors were used in this work (H. Erden, 2016; L. Erden, 2016). The Methane and Carbon Dioxide adsorption isotherm data on BPL-activated carbon adsorbent, a commercial granular activated carbon (Calgon Co.), were extracted from previously published data at 298.15, 323.15, and 348.15 K and in the pressure range of 0 - 700 kPa. The experimental part can be found in the other works of the authors (H. Erden, 2016; L. Erden, 2016), in detail.

Isotherm Models

For later usage in a particular gas separation application, a reliable correlation of the adsorption equilibrium data is required. In this paper, the data from the experimental adsorption equilibrium have been correlated using Simple Langmuir (SL), Dual Process Langmuir (DPL), Three Process Langmuir (TPL), Toth, and Unilan models. For each model, the temperature-dependent equations and the main model equations, given in Table 1, were used to determine model adsorption loading values ($q_{i,model}$) corresponding to each partial pressure. By simultaneously regressing all of the experimental single-gas data acquired at each temperature and minimizing $\sum_{i=1}^n (q_{i,model} - q_{i,experimental})^2$ using MS Excel's Solver, the fitting parameters were produced.

The SL, DPL, and TPL models are three different versions of the Langmuir isotherm. When a gas is adsorbing on a heterogeneous adsorbent made up of two energetically distinct but homogenous sites, the DPL model is used to describe the process. The TPL model also explains the adsorption of a gas on an adsorbent made up of three homogenous but energetically distinct sites (Bhadra et al., 2011). On each site, it is assumed that the free energy of adsorbate-adsorbent is constant.

Table 1. Adsorption equilibrium model equations used in this paper.

Model	Main Equation	Dependent equations
SL	$q = \left(\frac{q^s b P}{(1 + b P)} \right)$	$b = b_o \exp\left(\frac{E}{T}\right)$
DPL	$q = \left(\frac{q_1^s b_1 P}{(1 + b_1 P)} \right)_{site\ 1} + \left(\frac{q_2^s b_2 P}{(1 + b_2 P)} \right)_{site\ 2}$	$b_j = b_{j,o} \exp\left(\frac{E_j}{T}\right)$
TPL	$q = \left(\frac{q_1^s b_1 P}{(1 + b_1 P)} \right)_{site\ 1} + \left(\frac{q_2^s b_2 P}{(1 + b_2 P)} \right)_{site\ 2} + \left(\frac{q_3^s b_3 P}{(1 + b_3 P)} \right)_{site\ 3}$	$b_j = b_{j,o} \exp\left(\frac{E_j}{T}\right)$
Toth	$q = \frac{q^s b P}{(1 + (b P)^t)^{1/t}}$	$b = b_o \exp\left(\frac{E}{T}\right)$ $t = t_o - \frac{t_t}{T}$
Unilan	$q = \frac{q_s}{2s} \ln\left(\frac{1 + b e^s P}{1 + b e^{-s} P}\right)$	$b = b_o \exp\left(\frac{\bar{E}}{RT}\right)$ $\bar{E} = \frac{E_{max} + E_{min}}{2}$ $s = \frac{E_{max} - E_{min}}{2RT}$

The SL, DPL, and TPL equations can be seen in Table 1. The parameter q_j^s is the saturation capacity and b_j is the affinity parameter on-site j . E_j is the adsorption energy of the gas and $b_{j,o}$ is the pre-exponential factor on-site j . T is the temperature and P is the absolute pressure (Table 1) (Bhadra et al., 2011).

The representation of the Toth and Unilan models can also be seen in Table 1. The parameters t and s represent the heterogeneity of the system for the Toth and Unilan equations. b and t are dependent on temperature for the Toth equation. For the Unilan equation, b and s values depend on the temperature (Do, 1998).

RESULTS and DISCUSSION

Five different adsorption isotherm models were applied to experimental CH₄ and CO₂ adsorption isotherm data. The experimental adsorption isotherms on BPL-activated carbon were reported corresponding to each adsorption model for easy comparison separately for detailed information. Figure 1 to Figure 5 show the adsorption isotherms for pure CH₄ and CO₂ on BPL activated carbon at 25, 50, and 75 °C between 0 and 700 kPa obtained after outgassing the sample overnight at 150 °C (H. Erden, 2016; L. Erden, 2016). Experimental data for both CH₄ and CO₂ gases exhibit a convex curvature of type-1 adsorption isotherm according to the IUPAC classification for all three temperatures under these conditions. The adsorption isotherm data were also fitted with 5 different adsorption isotherm models.

Log-log scale isotherms were also reported in order to check the precision of the measured isotherms. It can be seen from the log-log scale adsorption isotherms that all measured isotherm slopes are showing constant behavior at low pressures, Henry's law region.

Simple Langmuir (SL) adsorption isotherm model was applied to the experimental CH₄ and CO₂ adsorption data. The SL model fits in linear form and the logarithmic scale for both gases are shown in Figure 1. The logarithmic scale isotherms show detailed fitting performance in Henry's law region which can not be seen well in linear scale. The SL fitting parameters and coefficient of determination (R²) were given in Table 2 for the Simple Langmuir model. It can be seen from the R² values that the SL model is substantially fitting the experimental data.

The Dual Process Langmuir (DPL) adsorption isotherm model was applied on the experimental CH₄ and CO₂ adsorption data. The DPL model fittings concerning experimental data in linear form and logarithmic scale for both gases are shown in Figure 2. The DPL fitting performance in Henry's law region is obviously better compared to the SL model which can be seen in the log-log scale graphs of Figure 1 and Figure 2. The DPL fitting parameters and coefficient of determination (R²) were given in Table 3 for the Dual Process Langmuir model. It can be seen from the R² values that the DPL model is fitting the experimental data quite well.

Three Process Langmuir (TPL) adsorption isotherm model was applied to the experimental CH₄ and CO₂ adsorption data. The TPL model fittings with respect to experimental data in linear form and logarithmic scale for both gases are shown in Figure 3. The fitting performance in Henry's law region is the best for the TPL model compared to other Langmuir models (SL and DPL) which can be relatively seen in log-log scale graphs of Figure 1 to Figure 3. The TPL fitting parameters and coefficient of determination (R²) were given in Table 4. It can be seen from the R² values that the TPL model is perfectly matching the experimental data for both gases and all three temperatures.

The temperature-dependent Toth adsorption isotherm model was applied to the experimental CH₄ and CO₂ adsorption data. The Toth model fittings with respect to experimental data in linear form and logarithmic scale for both gases are shown in Figure 4. The fitting performance in Henry's law region is also quite well for the Toth model which can be seen in the log-log scale graphs of Figure 4. The Toth fitting parameters and coefficient of determination (R²) were given in Table 5. It can be seen from the R² values that the Toth model is fitting quite well the experimental data for both gases.

Another temperature-dependent adsorption isotherm model used in this study was the Unilan model. It was applied to the experimental CH₄ and CO₂ adsorption data. The Unilan model fittings with respect to experimental data in linear form and logarithmic scale for both gases are shown in Figure 5. The fitting performance in Henry's law region is pretty good for the Unilan model which can be seen in

the log-log scale graphs of Figure 5. The Unilan fitting parameters and coefficient of determination (R^2) were given in Table 6. It can be seen from the R^2 values that the Toth model is fitting quite well the experimental data for both gases.

Regarding the 5 different models applied to the experimental data, TPL, DPL, and Toth models gave the best fittings for both gases investigated. On the other hand, SL and Unilan models showed quite well-fitting performances.

Table 2. Fitting parameters of the Simple Langmuir model and R^2 for each temperature.

Gas	q^s	b^0	E	R^2	R^2	R^2
	mol *kg ⁻¹	kPa ⁻¹	K	(25°C)	(50°C)	(75°C)
CO ₂	7.210	4.318*10 ⁻⁷	2696.62	0.99680	0.99739	0.99699
CH ₄	4,227	2.161*10 ⁻⁷	2116.84	0.99839	0.99917	0.99953

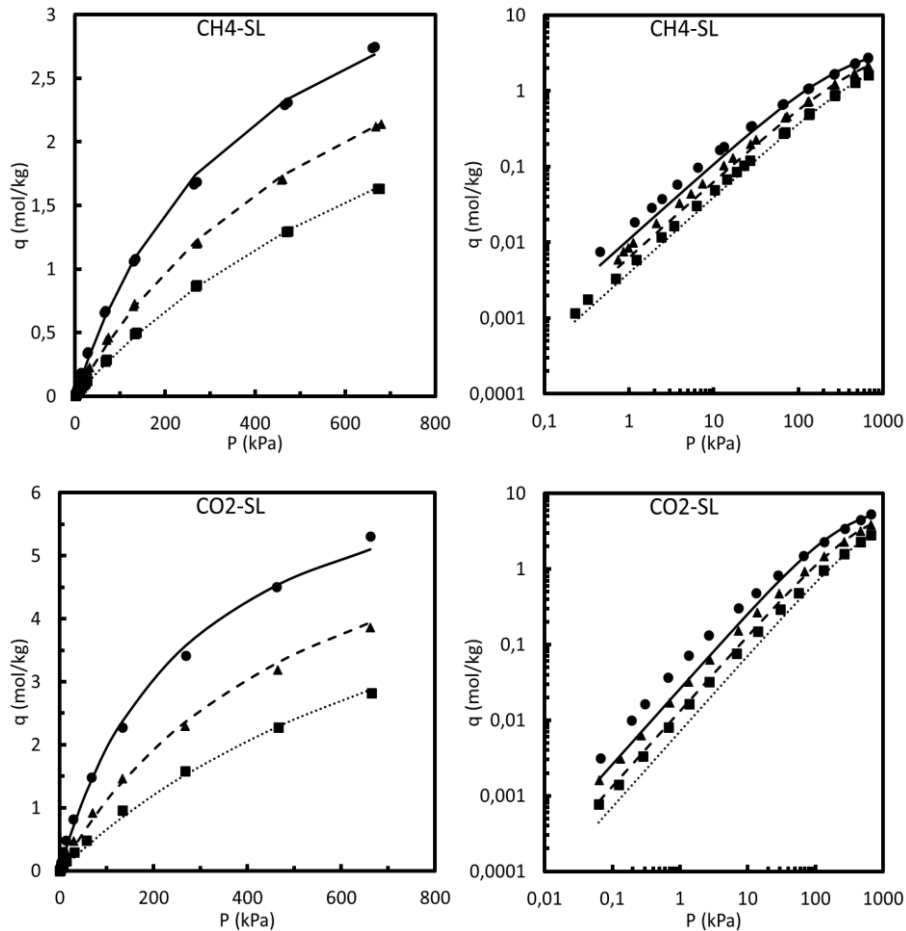


Figure 1. Simple Langmuir isotherm model fittings for adsorption isotherm data of CH₄ and CO₂ onto BPL-Activated Carbon at three different temperatures in linear (left), logarithmic scale (right). Solid circles for experimental data (25 °C), solid lines for the SL model (25 °C), Triangles for experimental data (50 °C), dashed lines for the SL model (50 °C), Squares for experimental data (75 °C), dotted lines for SL model (75 °C).

Table 3. Fitting parameters of the Dual Process Langmuir model and R^2 for each temperature.

Gas	q_1^s	b_1^0	E_1	q_2^s	b_2^0	E_2	R^2	R^2	R^2
	mol *kg ⁻¹	kPa ⁻¹	K	mol *kg ⁻¹	kPa ⁻¹	K	(25°C)	(50°C)	(75°C)
CO ₂	0,919	4,54E-07	3371,01	8,620	3,39E-07	2520,24	0,99998	0,99993	0,99993
CH ₄	0,543	6,73E-07	3040,38	5,092	2,02E-06	1901,02	1,00000	0,99999	0,99997

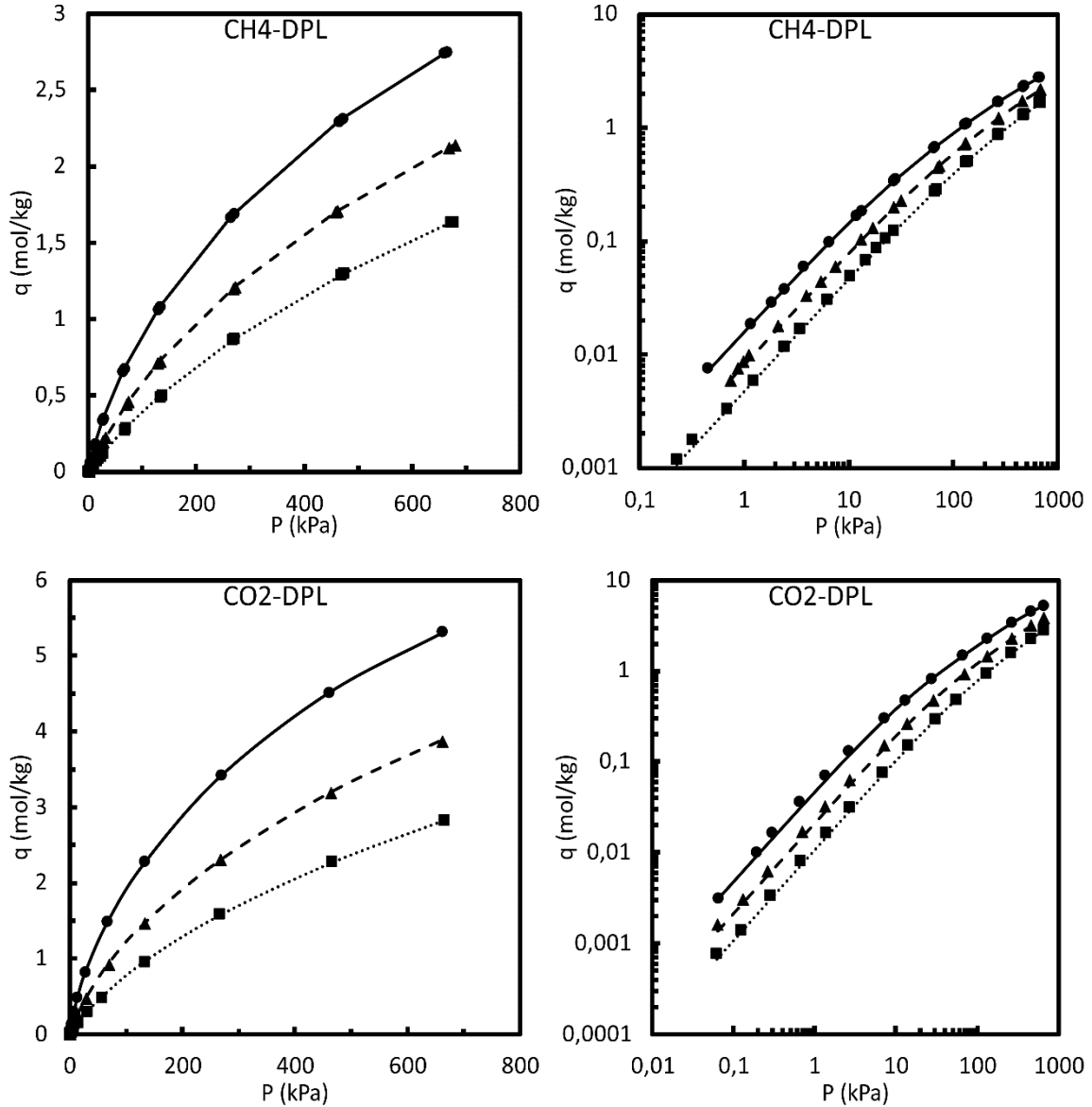


Figure 2. Dual Process Langmuir isotherm model fittings for adsorption isotherm data of CH₄ and CO₂ onto BPL-Activated Carbon at three different temperatures in linear (left), logarithmic scale (right). Solid circles for experimental data (25 °C), solid lines for the DPL model (25 °C), Triangles for experimental data (50 °C), dashed lines for the DPL model (50 °C), Squares for experimental data (75 °C), dotted lines for DPL model (75 °C).

Table 4. Fitting parameters of the Three Process Langmuir model and R^2 for each temperature.

Gas	q_1^0	b_1^0	E_1	q_2^0	b_2^0	E_2	q_3^0	b_3^0	E_3	R^2	R^2	R^2
	mol *kg ⁻¹	kPa ⁻¹	K	mol *kg ⁻¹	kPa ⁻¹	K	mol *kg ⁻¹	kPa ⁻¹	K	(25°C)	(50°C)	(75°C)
CO ₂	0,431	9,7E-08	4065,75	8,014	1,47E-07	2568,86	2,70	9,92E-07	2553,4	0,99999	0,99997	0,99997
CH ₄	0,537	6,73E-07	3042,90	2,027	2,02E-06	1896,535	3,05	2,02E-06	1907,6	1,00000	0,99998	0,99997

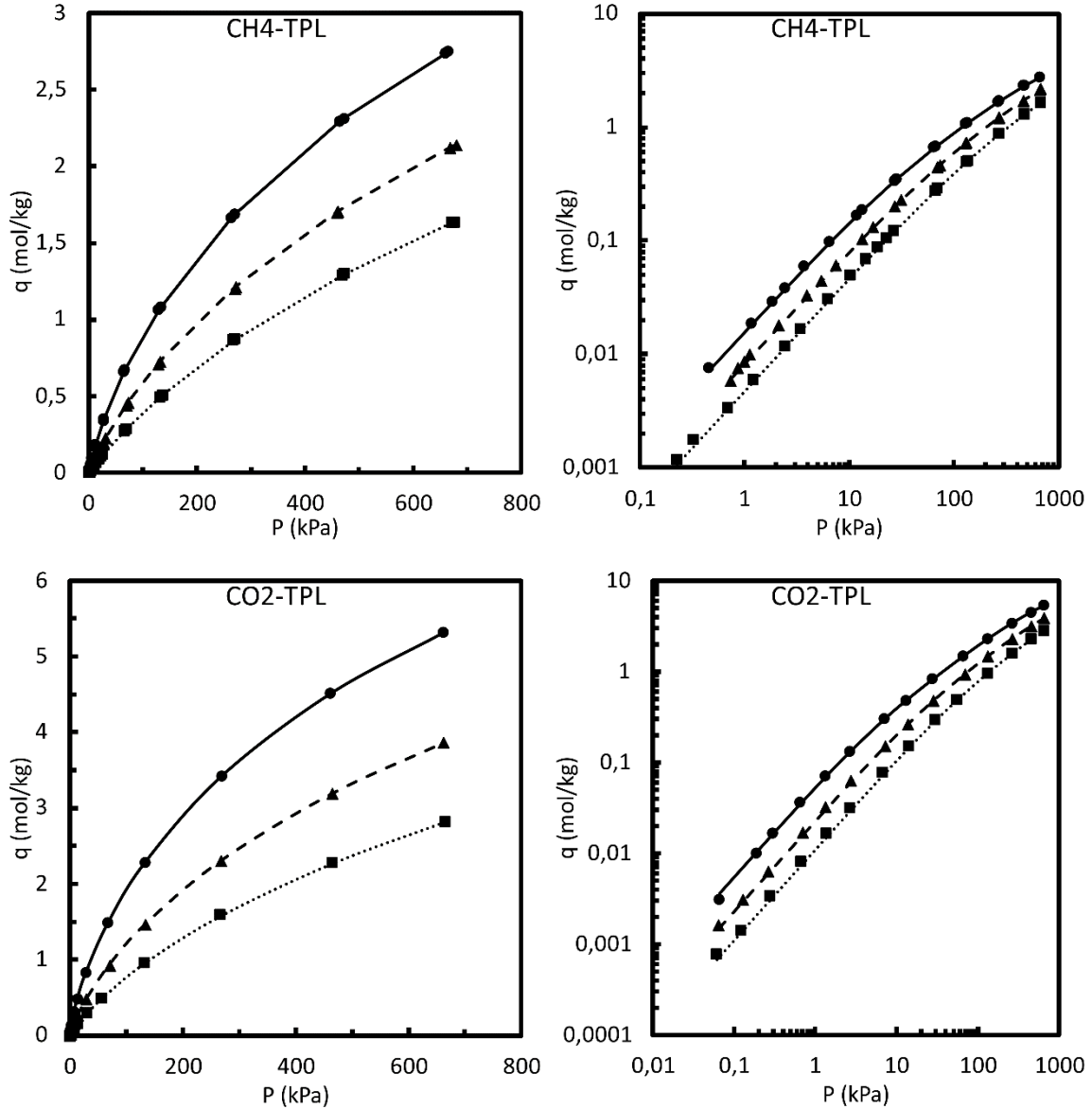


Figure 3. Three Process Langmuir isotherm model fittings for adsorption isotherm data of CH₄ and CO₂ onto BPL-Activated Carbon at three different temperatures in linear (left), logarithmic scale (right). Solid circles for experimental data (25 °C), solid lines for the TPL model (25 °C), Triangles for experimental data (50 °C), dashed lines for the TPL model (50 °C), Squares for experimental data (75 °C), dotted lines for TPL model (75 °C).

Table 5. Fitting parameters of the Toth model and R^2 for each temperature.

Gas	q^s	b_0	E	t_0	t_t	R^2	R^2	R^2
	mol *kg ⁻¹	kPa ⁻¹	K	-	K	(25°C)	(50°C)	(75°C)
CO ₂	20,669	5,01E-05	4,02E-07	2623,95	0,4217	0,99988	0,99993	0,99983
CH ₄	8,073	2,04E-06	1,89E-06	2059,72	0,5803	0,99983	0,99993	0,99975

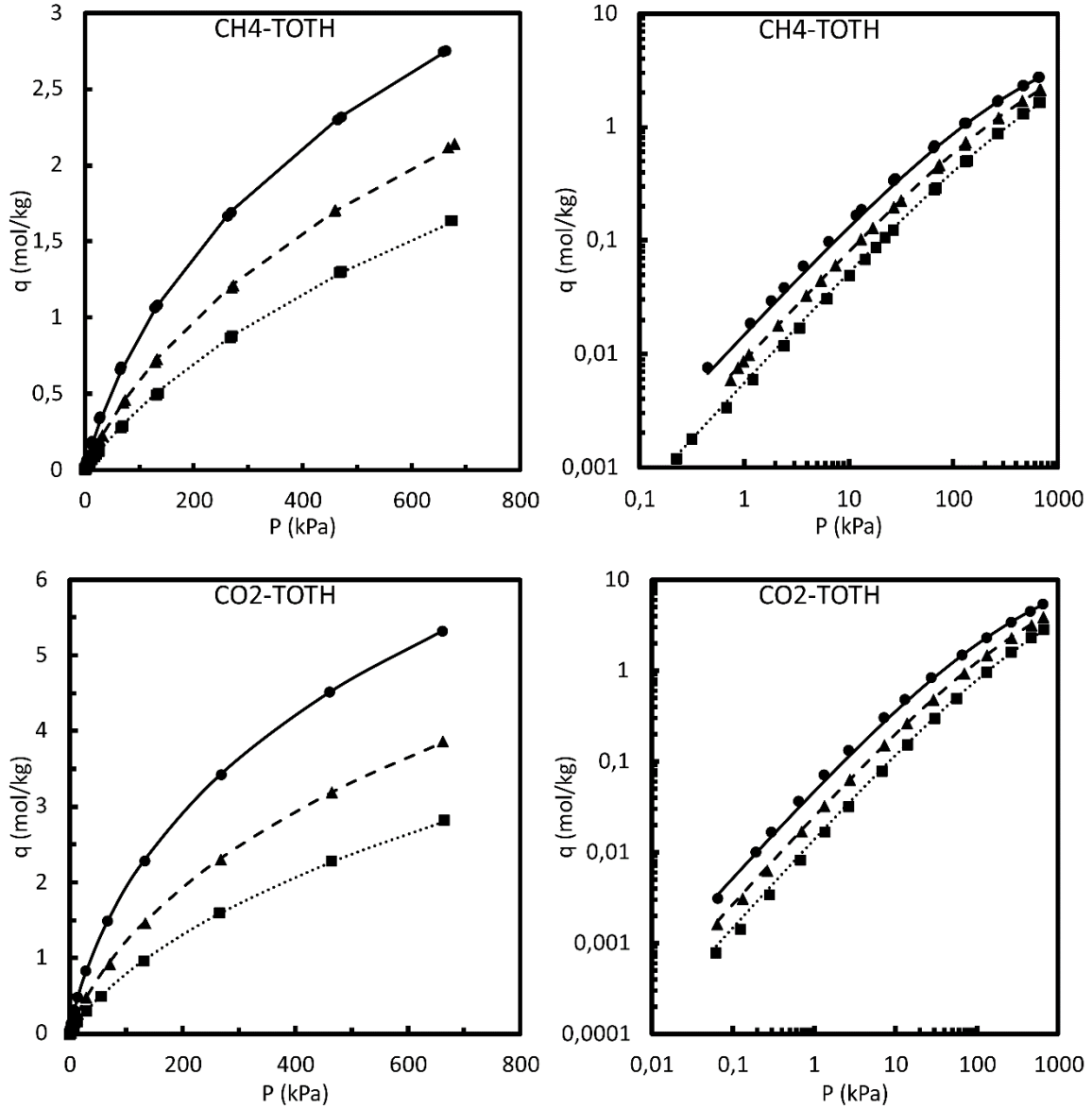


Figure 4. Toth isotherm model fittings for adsorption isotherm data of CH₄ and CO₂ onto BPL-Activated Carbon at three different temperatures in linear (left), logarithmic scale (right). Solid circles for experimental data (25 °C), solid lines for the Toth model (25 °C), Triangles for experimental data (50 °C), dashed lines for the Toth model (50 °C), Squares for experimental data (75 °C), dotted lines for Toth model (75 °C).

Table 6. Fitting parameters of the Unilan model and R^2 for each temperature.

Gas	q_s	b_0	E_{max}	E_{min}	R^2	R^2	R^2
	$mol \cdot kg^{-1}$	kPa^{-1}	$J \cdot mol^{-1}$	$J \cdot mol^{-1}$	(25°C)	(50°C)	(75°C)
CO ₂	19,57017	2,85E-07	26909,62	4675,87	0,99878	0,99894	0,99846
CH ₄	10,04359	1,5E-06	21570,75	3770,144	0,99950	0,99971	0,99979

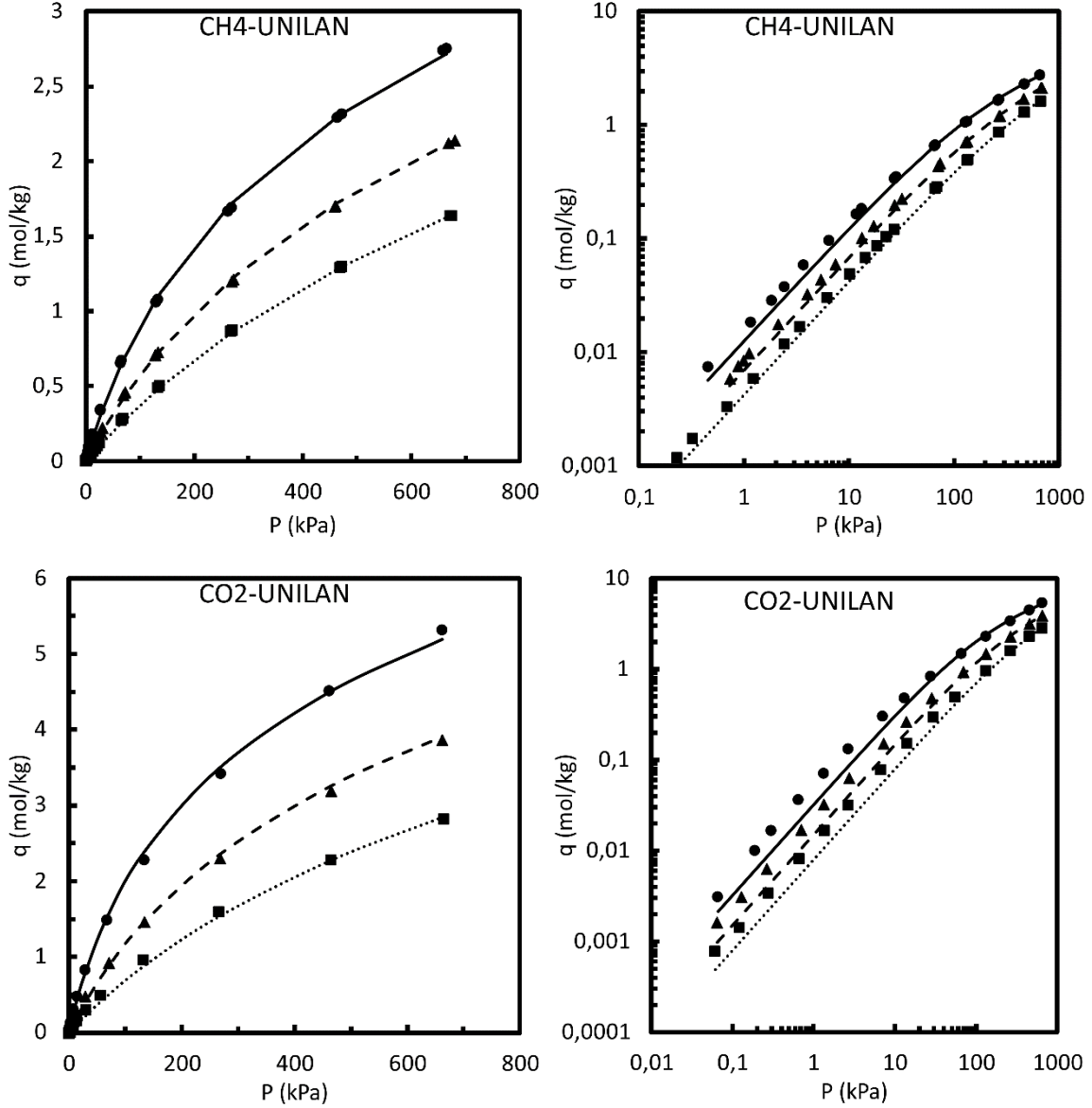


Figure 5. Unilan isotherm model fittings for adsorption isotherm data of CH₄ and CO₂ onto BPL-Activated Carbon at three different temperatures in linear (left), logarithmic scale (right). Solid circles for experimental data (25 °C), solid lines for the Unilan model (25 °C), Triangles for experimental data (50 °C), dashed lines for the Unilan model (50 °C), Squares for experimental data (75 °C), dotted lines for Unilan model (75 °C).

Conclusion

In this paper, we present 5 different adsorption isotherm model fittings for experimental CH₄ and CO₂ adsorption data on BPL-activated carbon for pressures ranging from 0 to 700 kPa and for temperatures ranging from 25°C to 75°C. DPL, TPL, and Toth models perfectly matched, whereas SL and Unilan models showed relatively good agreement with experimental data. Any adsorption-based separation modeling that uses BPL-activated carbon and CH₄-CO₂ gases can use the fitting parameter information offered in this article.

REFERENCES

- Belmabkhout, Y., Frère, M., & Weireld, G. De. (2004). High-pressure adsorption measurements. A comparative study of the volumetric and gravimetric methods. *Measurement Science and Technology*, 15(5), 848–858. <https://doi.org/10.1088/0957-0233/15/5/010>
- Bhadra, S. J., Ebner, A. D., & Ritter, J. A. (2011). On the use of the dual process Langmuir model for correlating unary equilibria and predicting mixed-gas adsorption equilibria. *Langmuir*, 27, 4700–4712. <https://doi.org/10.1021/la301004e>
- Chouikhi, N., Brandani, F., Pullumbi, P., Perre, P., & Puel, F. (2020). Biomethane production by adsorption technology: new cycle development, adsorbent selection and process optimization. *Adsorption*, 26(8). <https://doi.org/10.1007/s10450-020-00250-3>
- Dantas, T. L. P., Luna, F. M. T., Silva, I. J., de Azevedo, D. C. S., Grande, C. A., Rodrigues, A. E., & Moreira, R. F. P. M. (2011). Carbon dioxide-nitrogen separation through adsorption on activated carbon in a fixed bed. *Chemical Engineering Journal*, 169, 11–19. <https://doi.org/10.1016/j.cej.2010.08.026>
- Do, D. D. (1998). Adsorption Analysis: Equilibria and Kinetics. In *Chemical Engineering* (Vol. 2, Issue Imperial College Press). <https://doi.org/10.1142/9781860943829>
- Dolan, W. B., & Michael J. Mitariten. (2003). *CO2 rejection from natural gas*.
- Erden, H. (2016). *Two-Stage Psa System For CO2 Removal And Concentration During Closed-Loop Human Space Exploration Missions*. University of South Carolina.
- Erden, L. (2016). *Methane Separation And Purification Via Pressure Swing Adsorption*. University of South Carolina.
- Fouladi, N., Makarem, M. A., Sedghamiz, M. A., & Rahimpour, H. R. (2020). CO₂ adsorption by swing technologies and challenges on industrialization. In *Advances in Carbon Capture: Methods, Technologies and Applications*. <https://doi.org/10.1016/B978-0-12-819657-1.00011-6>
- Ho, Y. S., Porter, J. F., & McKay, G. (2002). Equilibrium isotherm studies for the sorption of divalent metal ions onto peat: Copper, nickel and lead single component systems. In *Water, Air, and Soil Pollution* (Vol. 141, Issues 1–4). <https://doi.org/10.1023/A:1021304828010>
- Park, J., Rubiera Landa, H. O., Kawajiri, Y., Realff, M. J., Lively, R. P., & Sholl, D. S. (2020). How Well Do Approximate Models of Adsorption-Based CO₂ Capture Processes Predict Results of Detailed Process Models? *Industrial and Engineering Chemistry Research*, 59(15). <https://doi.org/10.1021/acs.iecr.9b05363>

- Reynolds, S. P., Ebner, A. D., & Ritter, J. A. (2006). Enriching PSA cycle for the production of nitrogen from air. *Industrial & Engineering Chemistry Research*, 45(9), 3256–3264. <https://doi.org/10.1021/ie0513550>
- Ribeiro, A. M., Grande, C. A., Lopes, F. V. S., Loureiro, J. M., & Rodrigues, A. E. (2008). A parametric study of layered bed PSA for hydrogen purification. *Chemical Engineering Science*, 63, 5258–5273. <https://doi.org/10.1016/j.ces.2008.07.017>
- Ruthven, D. M., Farooq, S., & Knaebel, K. S. (1994). Pressure swing adsorption. In *VCH Publishers: New York*.
- Santos, J. C., Cruz, P., Regala, T., Magalha, F. D., Mendes, A., & Engenharia, F. De. (2007). High-purity oxygen production by pressure swing adsorption. *Industrial & Engineering Chemistry Research*, 46(2), 591–599.
- Sircar, S., & Golden, T. C. (2000). Purification of Hydrogen by Pressure Swing Adsorption. *Separation Science and Technology*, 35(5), 667–687. <https://doi.org/10.1081/SS-100100183>
- Sircar, S., Golden, T. C., & Rao, M. B. (1996). Activated carbon for gas separation and storage. *Fuel and Energy Abstracts*, 34(1), 1–12. [https://doi.org/10.1016/0140-6701\(96\)89610-X](https://doi.org/10.1016/0140-6701(96)89610-X)
- Tagliabue, M., Farrusseng, D., Valencia, S., Aguado, S., Ravon, U., Rizzo, C., Corma, A., & Mirodatos, C. (2009). Natural gas treating by selective adsorption: Material science and chemical engineering interplay. *Chemical Engineering Journal*, 155, 553–566. <https://doi.org/10.1016/j.cej.2009.09.010>
- Toth, J. (1971). State Equations of Solid-Gas Interface Layers. *Acta Chimica Academiae Scientiarum Hungaricae*, 69(3).
- Yang, R. T. (1997). Gas Separation by Adsorption Processes. In *Imperial College Press: London*. Imperial College Press. [https://doi.org/10.1016/0950-4214\(88\)80042-2](https://doi.org/10.1016/0950-4214(88)80042-2)